Int J Adv Manuf Technol (2014) 71:1511–1523
DOI 10.1007/s00170-013-5570-0

ORIGINAL ARTICLE

Tool wear and hole quality investigation in dry helical milling of Ti-6Al-4V alloy

Hao Li · Gaiyun He · Xuda Qin · Guofeng Wang · Cui Lu · Linjing Gui

Received: 15 June 2013 / Accepted: 16 December 2013 / Published online: 12 January 2014

Abstract This paper focused on combined study on the evolution of tool wear and its influence on borehole quality in dry helical milling of Ti-6Al-4V. The carbide tools with TiAlN coating were used in this experimental investigation. The tool wear characteristics both at front and periphery cutting edges were investigated using an optical microscope and SEM-EDS techniques. The experimental results demonstrate that the combined effects of chipping/fracture, diffusion, and oxidation have significant bearings on front cutting edge failure, while the flank wear was predominant at the periphery cutting edges. The cutting speed was correlated with tool failure mechanizes, and the different wear rates at front and periphery cutting edge caused different variation trends of cutting force in thrust and horizontal direction during hole-making process. The quality of machined holes was evaluated in terms of geometry accuracy, burr formation, and surface roughness. The exit-burrs of machined hole were closely correlated with front cutting edge wear. However, high hole quality was observed even the near end of tool life from the point of view of diameters, roundness error, and surface finish due to the smooth wear pattern at periphery cutting edges. Severe tool wear at front cutting edges will cause excessive exit-burrs, but it has no obvious effect on geometry and surface roughness in helical milling of Ti-6Al-4V.

Keywords Helical milling · Dry machining · Tool wear · Ti6Al4V · Hole quality

H. Li · G. He · X. Qin (✉) · G. Wang · C. Lu · L. Gui
Key Laboratory of Mechanism Theory and Equipment Design of Ministry of Education, Tianjin University, Tianjin 300072, China
e-mail: qxd@tju.edu.cn

1 Introduction

Due to high strength-to-weight ratio and excellent resistance, titanium and titanium alloys are excellent candidates for high performance applications [1]. However, tool wear in titanium alloy machining process is severe because of high cutting temperature and low thermal conductivity [2]. In the machining process, high cutting temperature also enhances the chemical reactivity of titanium, producing a strong adhesion of the workpiece to tool surface and leading to premature tool failure [3]. Kramer [4] separated the wear into a low-temperature region wear (the mechanical wear like abrasion is predominant) and a high-temperature region wear (chemical properties and diffusion are the predominant). Tool wear in machining of titanium alloys is mainly caused by high cutting temperature in the vicinity of cutting edges, and in addition, adhesion-dissolution-diffusion wear, attrition, and micro- and macro-fracturing of the cutting edge also increase the risk of rapid tool wear [5]. In this paper, the tool wear in helical milling of Ti-6Al-4V alloy was been studied separately from front cutting edge and periphery cutting edge under dry machining condition.

The cutting temperature in cutting zone mainly depends on the cutting speed and cutting force. Several authors developed experimental techniques to study on the progressive tool failure during machining operations. The cutting speed and cutting force are two important factors needed to consider in the investigation of tool wear. It can achieve a more realistic optimization of machining operations by building the relationship between process factors and tool degradation. Wanigarathne et al. [6] established the interrelationships between the progressive tool wear, cutting temperature, and the cutting forces experimentally. Zhang et al. [7] have analyzed the tool wear and the cutting force variation during high-speed end milling of Ti-6Al-4V alloy.

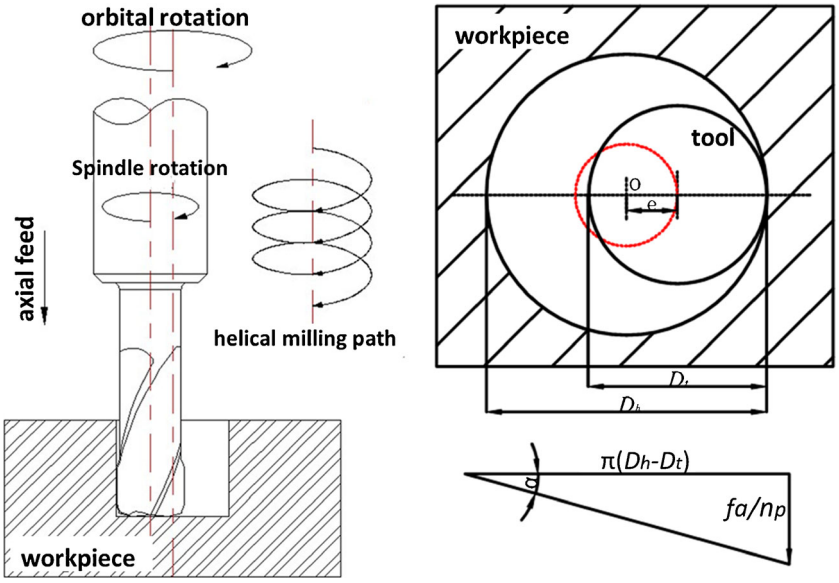

Fig. 1 Helical milling kinematics

Mantle et al. [8] have studied on the effects of machining parameters in relation to tool life, hole quality, and cutting force and workpiece surface integrity. The cutting speed was correlated with progressive tool failure mechanisms, and the different conditions of friction and normal stresses caused by different cutting forces and cutting temperatures under different cutting speeds resulted in varieties of progressive tool wear mechanisms [9]. At the same time, finite element method has been utilized to investigate the machining of Ti-6Al-4V alloy in high cutting speed range [10–12], but it is still difficult to discuss the tool wear and cutting force and the coated carbide tools under a certain flank wear. Furthermore, the above research results did not involve the relationship between the tool wear mechanism and process factors (cutting force and cutting speed) in Ti-6Al-4V helical milling.

As one of the new hole-machining methodologies, helical milling has a number of advantages such as smooth cutting process, small thrust force, and high accuracy compared with conventional drilling. Due to the excellent performance in hole-making operations, the helical milling process is widely researched, especially for difficult-to-cut materials, such as titanium alloy and carbon fiber reinforced plastic (CFRP) [13]. Detailed studies about helical milling process have been initiated. Iyer et al. [14] proved that helical milling is capable of machining H7 quality holes with a surface finish of 0.3 μm Ra in AISI D2 tool steel. Denkena et al. [15] investigated the influence of the axial and tangential feed on cutting forces and borehole quality during helical milling of layer compounds consisting of unidirectional CFRP and Ti-6Al-4V. Brinksmeier et al. [16] established the mathematical model of helical milling kinematics to describe mathematically the occurring cutting conditions over the engagement angle as a function of the parameters: hole diameter, tool diameter, and gradient of the helical course. Based on an improved Z-map model, a 3D surface topography simulation model was established to simulate the surface finish profile in helical milling process [17]. Wang et al. [18] established an analytical cutting force model of the helical milling which can be utilized to predict the change of cutting force in helical milling process under different cutting conditions. Nevertheless, the detailed study about tool wear mechanism of helical milling process was not elaborated clearly.

Titanium alloys represent a significant metal portion of aircraft structural and engine components. In order to meet the requirements of low costs of production and safe assembly environment, the dry cutting is recommended by aeronautical manufacturers. Several papers about machining titanium alloy with dry cutting [19, 20] have been published. Dry machining of titanium alloys is difficult because the temperature at the cutting edge is very high, and it should be controlled to guarantee the quality of machined hole. When these critical structural components in aerospace industry

Table 1 The cutting parameters for helical milling Ti-6Al-4V

Cooling condition	Cutting speed	Tangential feed	Axial feed	Hole diameter	Hole depth	Axial distance of tool machined
Dry	120/100/80/60 m/min	0.04 mm/tooth	0.2 mm/rev	10 mm	10 mm	12 mm

Table 2 Nominal composition of alpha-beta Ti-6Al-4V (weight percent)

Al	V	Fe (max)	Si (max)	C (max)	N (max)	H (max)	O (max)	Titanium
5.5–6.8	3.5–4.5	0.3	0.15	0.1	0.05	0.015	0.15	Balance

are manufactured with the objective to reach high reliability levels, surface integrity is one of the most relevant factors for evaluating the quality of machined surfaces. Herberta et al. [21] made an evaluation of the evolution of workpiece surface integrity in hole-making operations (plunge milling and drilling) for a nickel-based superalloy, while Sharman [22] presented the tool life and surface integrity aspects when drilling and hole making in Inconel 718. Biermann et al. [23] presents the influence of tool geometry, coating, and cutting data on the bore hole quality.

Most of these papers focused on the conventional drilling process, and there is few study about the hole quality of helical milling published. Machining of titanium alloys will cause rapid chipping at the cutting edge which could lead to catastrophic tool wear of the inserts [24]. Tool wear is an important factor which affects the borehole quality. In this paper, the evolution of tool wear and the correlations between the cutting speed with tool degradation for dry helical milling Ti-6Al-4V were analyzed. Moreover, the influence of tool wear on the quality of machined hole in dry helical milling of Ti-6Al-4V with carbide tools was also presented.

2 Experimental

The helical milling feed was realized by motion compensation of machining center. The detailed helical milling kinematics is shown in Fig. 1. As shown in the figure, the borehole is generated by a milling tool which executes a helical path in the workpiece. The three motions in helical milling process are orbital rotation, spindle rotation, and axial feed. To establish the relationship of helical milling parameters, the following variables are used: D_t, tool diameters (millimeters); D_h, borehole diameters (millimeters); n, spindle rotation speed (rpm); n_p, orbital rotation speed (rpm); and a, feed rate in axial direction per orbital rotation (millimeters per revolution).

The angular velocities corresponding to spindle rotation and orbital rotation can be given as follows:

$$\omega = 2n\pi/60;\ \omega_p = 2n_p\pi/60 \tag{1}$$

$$f_a = a \times n_p \tag{2}$$

$$\alpha = \arctan(f_a/(\pi \times (D_h - D_f) \times n_p)) \tag{3}$$

The cutting parameters in the experiment are shown in the Table 1, and the axial feed represents the axial feed per orbital revolution. The axial distance of the tool machined in every hole-making operation was 12 mm, and the thickness of titanium plate was 10 mm. Therefore, it can make sure that all holes are through-hole in this experimental study. The alpha-beta titanium alloy Ti-6Al-4V plates was used as workpiece materials in this study, and the nominal chemical composition of Ti-6Al-4V is shown in Table 2.

In tool wear investigation under the variation of cutting speed, tool rejection or failure was determined based on the following criteria:

1. Average nonuniform flank wear VB = 0.2 mm;
2. Maximum flank wear VBmax = 0.3 mm;
3. Excessive chipping/flaking or catastrophic failure.

The experiment trial will be stopped when any one of the above criteria is reached.

In this paper, helical milling operations were performed on DMC75Vlinear five-axis high-speed machining center. As shown in Fig. 2, a Kistler three-direction stationary dynamometer (9257A) and supporting Kistler charge amplifier (type 5070) were used, and data acquisition board and Kistler software were utilized for a three-direction cutting force measurement. The tools specifically designed for helical milling were used in this study, as shown in Fig. 2. The ultrafine grain carbide helical milling tools (ISO K10) recommended by tool manufacturers were selected for helical milling tests. The composition of the cutter matrix is WC-8 % Co, and the thickness of the TiAlN coating is 1∼3 μm.

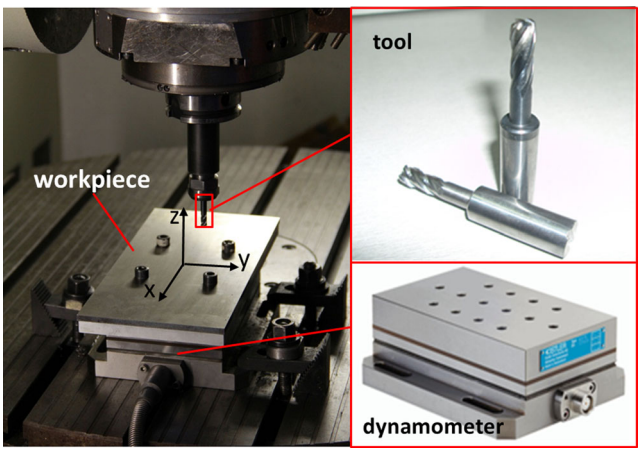

Fig. 2 Experimental setups and helical milling cutters used in the experiment

Table 3 The parameters for helical milling cutter

Diameter of cut	Length of cut	Length overall	First clearance angle	Second clearance angle	Number of teeth
6 mm	4 mm	55 mm	15°	20°	4

The detailed parameters of helical milling tool used in this paper are shown in Table 3.

The observation of tool wear mechanism was carried out using a scanning electron microscope (SEM), Philips XL-30 with an EDSDX4i system. The further investigation about elemental distribution was performed using energy-dispersive X-ray (EDX). The tool wear observation was carried out by a SI-DUSB-8-1300k digital camera after each hole was machined. The measurement of diameter accuracy and roundness error was achieved using coordinate measuring machine (CMM), and the surface roughness values were obtained by Talysurf of Taylor Hobson surface profilers.

3 Results and discussion

3.1 Tool wear

The helical milling process is completely different from other hole-making processes; the front cutting edges and the periphery cutting edge all take part in the machining process at the same time. The periphery materials of the borehole are removed by the periphery cutting edges, and the part of material at the bottom of borehole is removed by front cutting edges [16]. Therefore, in this paper, the tool wear of helical milling was separately investigated in the following three zones: front cutting edges zone, periphery cutting edges zone, and the tool nose. These three zones are marked with A (tool nose), B (front cutting edge), and C (periphery cutting edge) in Fig. 3. All the experiments were carried out under the dry condition with the specially designed helical milling tools, and cutting parameters are shown in Table 1.

3.1.1 Front cutting edge wear

Figure 4 is the photography of initial wear of the front cutting edge zone after machining three holes (cutting time with 2.5 min). Image shows that the clearance face near the cutting edges presents the different color contrasts. Zones with different contrasts were analyzed by EDX technique, and the results show that the bright white region corresponds to tool substrate (WC-8 % Co) and coating materials (TiAlN); the gray region only corresponds to coating materials (TiAlN). The above results suggest that part of coating material has been removed. However, the geometry parameters of the cutter were measured by an optical microscope, and no significant changes were observed at the front cutting edges.

With the increase of cutting time, the phenomena described in the initial phase of tool wear showed increase in evolution. It is observed that more coating materials were lost compared with initial wear stage. The medium wear situation of front cutting edge zone after a cutting time of 12.5 min is shown in Fig. 5a. It is interesting to observe that the early chipping/fracture firstly occurred at the tool nose in general (the zone which is marked with A in Fig. 3). The main occurrence reason of this phenomenon is the highest cutting speed, and the cutting temperature [19] was reached compared with other positions at the front cutting edges in helical milling process. Furthermore, the helical milling process consists of a discontinuous milling process on the periphery cutting edge and a continuous drilling process on the front cutting edge [15]. The tool noses are subject to thermal cycles owing to discontinuous cut, and it will increase the wear rate to a certain extent. Chipping at the tool nose would lead to flaking with the cutting time increases, as shown in Fig. 5c. Although these flaking do

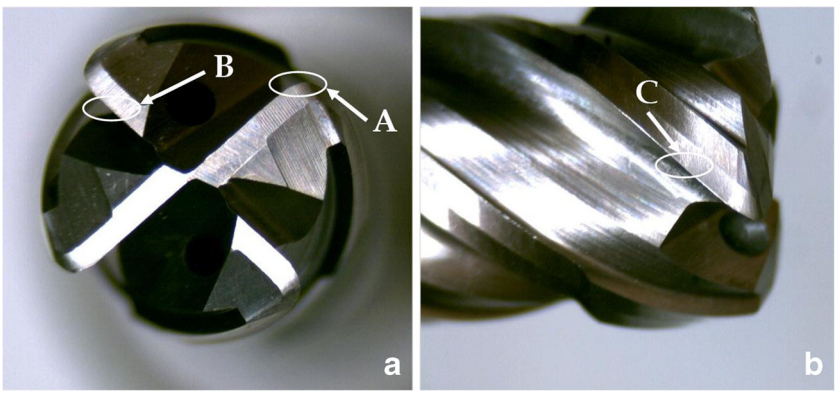

Fig. 3 Three sections of interest in wear mechanism study on helical milling

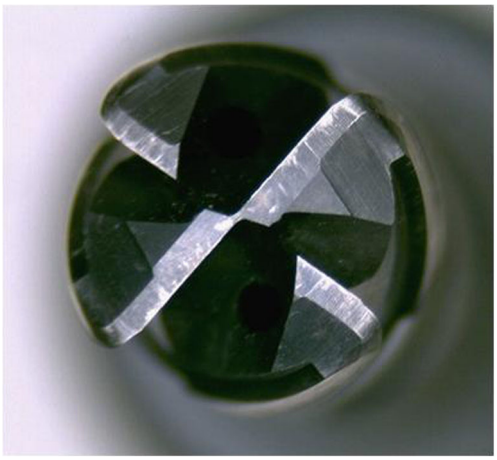

Fig. 4 Initial wear of the bottom cutting edge zone after machining three holes (cutting time 2.5 min)

not affect the surface quality of the machined hole, they weaken the tool [25]. When the tripping/fracture occurred, the cutting force will increase due to the change of geometry parameters, and the more tough cutting condition will be present for the cutting tool and lead to more serious wear.

Figure 5b shows an image of the front cutting edge when cutting time reached 12.5 min. The good geometry shape of the front cutting edge was still obtained. However, the adhesion phenomena were observed as shown in the figure. The adhesion phenomena are formed due to the high pressure generated during cutting and the high chemical affinity of the tool to the workpiece material. Sharman et al. [26] has made similar observations in end milling of Inconel 718TM. When ball nose-end milling Inconel 718, they found that the main wear mechanism was adhesion and reported built-up edge (BUE) formation and plucking of the tool coating. When adhesion materials is taken off during the machining process, the fresh tungsten carbide substrate is easily exposed, decreasing the strength of the tool and leading to the rapid wear, such as craters. As shown in Fig. 5d, small crater was observed at the front cutting edge when the cutting time reached 18.3 min. Because the cemented carbide belongs to the brittle material, brittle tripping is very common in the Ti-6Al-4V helical milling process.

The EDX analysis result of worn front cutting edge is shown in Fig. 6, and two kinds of wear mechanism were observed through the results of SEM-EDX: diffusion and adhesion. According to Nabhani [27], the temperature of the cutting zone even at moderate cutting velocity is generally around 900 °C. At such high temperature, the titanium chip maintains a very high intimate contact with the tool rake and flank face especially at the condition with no protection of coating. The EDX analysis of the crater (spectrum A) proved that the diffusion wear exists in the crater section. In the spectrum, peaks of W and Co correspond to the tool substrate, while peaks of Ti corresponds to the workpiece materials. The diffusion between the cemented carbide tool and titanium alloys can embrittle the region of tool where diffusion happened [28]. The diffusion speed of carbon atoms from tool substrate is more rapid than metal atoms (Co and W) [19]. A carbon-deficient region appeared at the tool subsurface, and this may be the reason for the embrittlement of the tool. This process may lead to the more

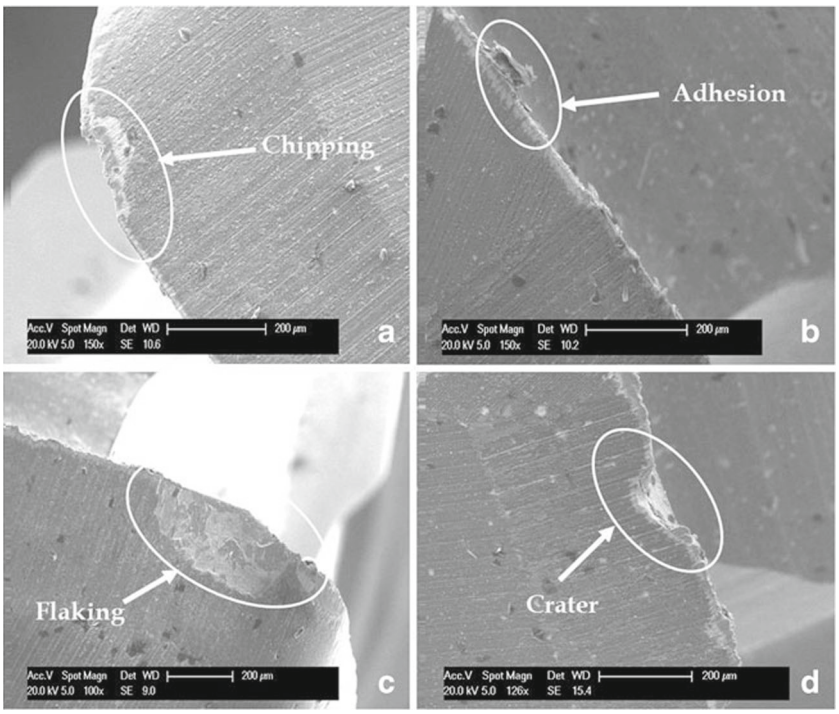

Fig. 5 Medium wear of front cutting edge: **a** chipping at cutting time of 12.5 min, **b** adhesion at the cutting time of 12.5 min, **c** flaking at the cutting time of 18.3 min, and **d** crater at the cutting time of 18.3 min

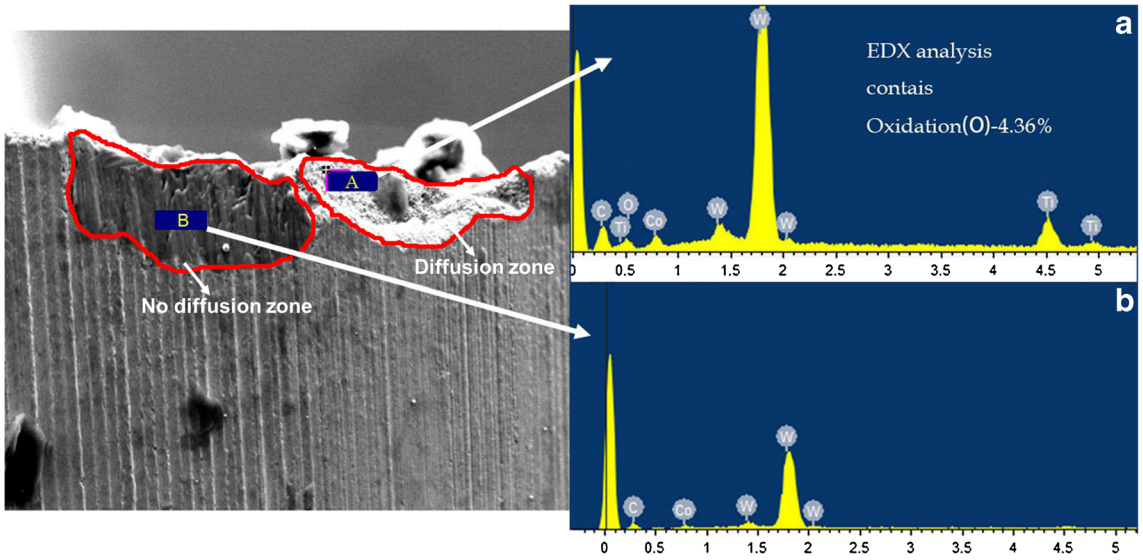

Fig. 6 EDX analysis of bottom cutting edge zone (cutting time of 22.5 min)

serious brittle chipping/fracture. As shown in Fig. 6, chipping/fracture was observed at the diffusion zone of front cutting edges. It is interested to find that oxidation mechanism that occurred during the dry helical milling process (spectrum A). Therefore, the combined action of diffusion, adhesion and oxidation generates the craters shown in Fig. 6. The flaking wear pattern was also observed in section B; the EDX result is shown in the spectrum B and no diffusion or adhesion occurred in section B.

According to Astakhov [29], machining of difficult-to-machine materials and in high-speed machining, plastic lowering of the cutting edge is the predominant cause of premature tool failure. In the machining process, the stress concentration at the cutting edge trends to deform the tool edge plastically. Because the chipping/fracture occurred more easily and played a predominant role in wear process, the plastic lowing phenomenon is not observed in the current study. As shown in Fig. 7, the more severe crater was also observed at the tool nose. EDX analysis of the crater was carried out, and the results are similar to the result of spectrum A in Fig. 6.

At the end of the tool life, the excessive chipping and fracture occurred in the cutting edge. The catastrophic fracture was observed at one of the tool noses (this region may reach the highest cutting temperature and cutting speed in helical milling process), as shown in Fig. 8a. However, the rest of cutting edges did not show significant change in geometry. The fractures were also observed at the other position of front cutting edge (Fig. 8b). High stress and cutting temperatures coupled with the brittleness of the substrate tool due to diffusion may accelerate the chipping, flaking, cracking, and fracture of the tool [30]. Catastrophic failure of the tool occurred without previous progressive

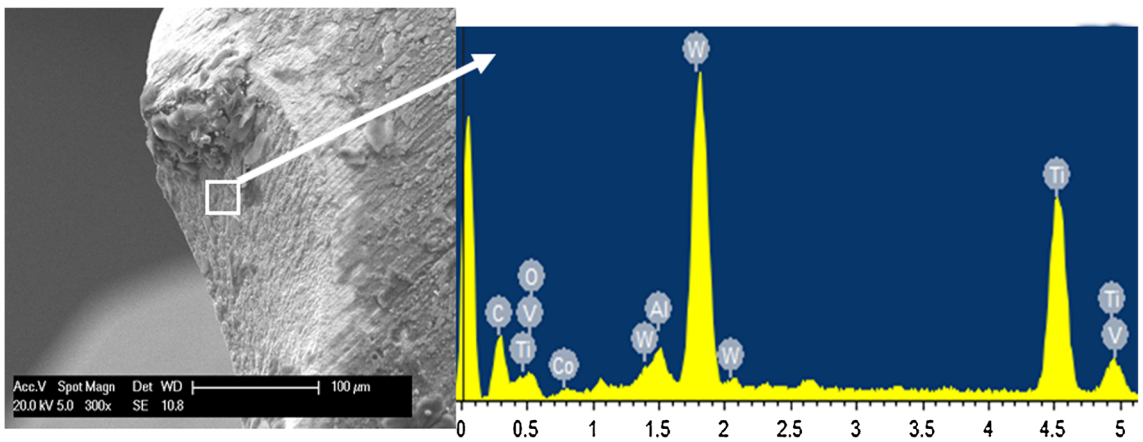

Fig. 7 EDX analysis of cutter nose (cutting time of 22.5 min)

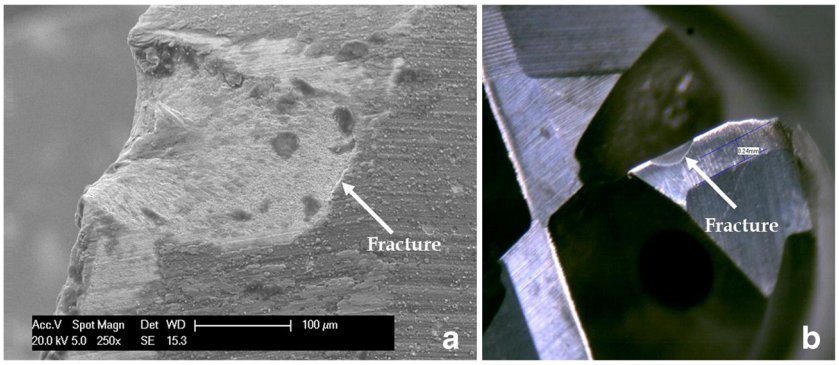

Fig. 8 Final wear of front cutting edge zone: **a** fracture at tool nose (cutting time 33.3 min) and **b** fracture at cutting edge (cutting time 33.3 min)

wear. The tool life in this test is mainly decided by the wear performance of front cutting edges.

3.1.2 Periphery cutting edge zone wear

It is interested to find that the wear at the periphery cutting edge zone is not quite severe compared with the front cutting edge, and the occurrence time of obvious wear is much later. As shown in Fig. 9a, the coating material (TiAlN) in the vicinity of the periphery cutting edges was lost at the rake face of the periphery cutting edges when machined for 5 min, but no significant geometry change was observed. The loss of coating leads to the weakness at the cutting edges, and the flaking and chipping/fracture were followed with the increase of cutting time, as shown in Fig. 9b, c. Different from the chipping/fracture that occurred at the front cutting edge, the process that occurred at the periphery cutting edge was the predominate reason to affect the surface quality of the machined hole.

Micro-craters were also observed at the periphery cutting edges at the cutting time of 23.3 min, as shown in Fig. 9. The wear mechanism is similar to the mechanism at the front cutting edges, in which diffusion and adhesion were also observed using the EDX analysis method. The different point comparing with front cutting edge wear is smooth, and steady wear was widely observed at the periphery cutting edge (Fig. 10). This might be due to the following two facts: abrasion wear was more predominant than other wear mechanisms on the flank face of the periphery cutting edges, and better cutting environment (both in cutting heat and cutting force) is presented due to the unique characteristic in helical milling process. The interrupted and eccentrically machining process elevates the room for chip removing and heat flowing.

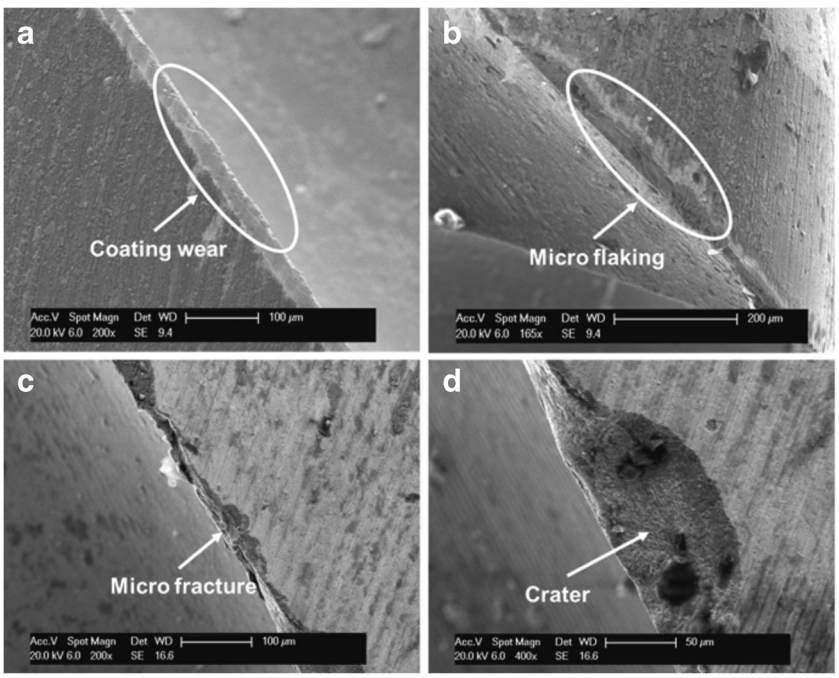

Fig. 9 The wear process of the periphery cutting edge: **a** coating materials lost at flank face (cutting time 5 min), **b** micro-flaking that occurred at the cutting edge (cutting time 12.5 min), **c** micro-chipping/fracture that occurred at the cutting edge (cutting time 18.3 min), and **d** micro-crater at the cutting edge (cutting time 23.3 min)

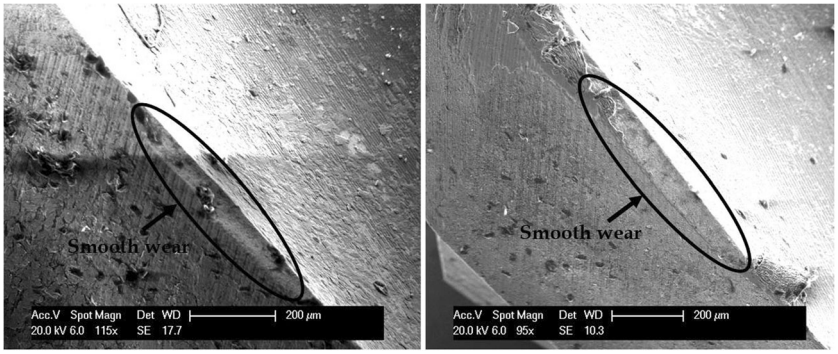

Fig. 10 Smooth wear at flank face of the periphery cutting edge zone (cutting time 33.3 min)

According to the above observation results of the tool wear process both at the front cutting edge and periphery cutting edge, micro-smooth wear (Fig. 11) was predominant at the periphery cutting edge when the excessive fracture or crater (as shown in Figs. 7 and 8) occurred at the front cutting edge. The cutting forces have a strong positive correlation with the tool wear propagation. When the chipping and fracture occurred, the cutting force will increase due to the change of tool geometry parameters and sharpness. As shown in Fig. 11, the variation of cutting force in helical milling process is presented. The cutting force of Fx (or Fy) , which is the cutting force in horizontal direction, is lower than the thrust force in helical milling process and has no obvious fluctuation with increasing cutting time. However, the thrust cutting force increases with the progression of tool wear, which ranges from 115 to 257 N as shown in Fig. 11. That is to say, tool wear in helical milling process only has influence on the variation of thrust force but has little influence on the cutting force of Fx (or Fy). In the helical milling process, the cutting force in thrust and horizontal directions mainly depend on the tool wear of the front and periphery cutting edge, respectively. Therefore, the different wear characteristics in helical milling tool—excessive chipping/fracture at front cutting edge and micro-flank wear at periphery cutting edge—will lead to the different variation trends of cutting force.

3.1.3 Effect of cutting speed variation on tool wear progression

The developments of flank wear obtained for helical milling with coated carbide tools operated at various cutting speeds are shown in Fig. 12. The tool life for hole-making process can be replaced by borehole numbers. With the increase of machined hole numbers, the average flank wear of the front cutting edges increased gradually when the cutting speeds were lower than 100 m/min. However, it was found that when higher cutting speed was employed, the tool wore quite rapidly. The tool life of hole making was less than 14 holes when the cutting speed was 120 m/min. The number of machined hole increased almost six times when the lower cutting speed (60 m/min) was used. The failure mode images when the tool reached the tool life criteria under various cutting speeds are shown in Fig. 13. Catastrophic failure is a common failure mode under the cutting speeds of 120 and 100 m/min, while it turns out to be the flank wear or nonuniform flank wear under the lower cutting speed (60 and 80 m/min).

For metal machining process, the cutting temperature became higher with the increase of cutting speed. Due to the low thermal conductivity of titanium alloy, high cutting temperature is generated at the tool-chip contact zone, especially at the tool nose. The three causes of tool failure are qualitatively presented in Fig. 14, including

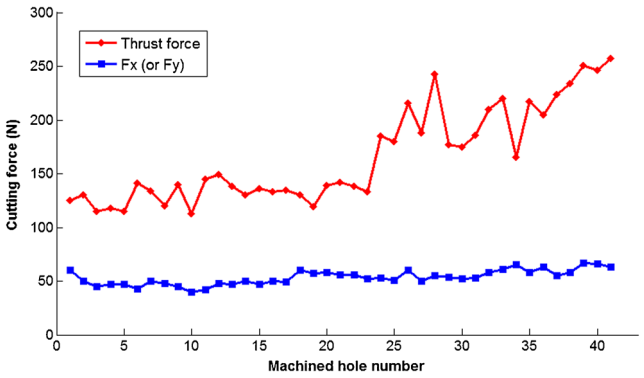

Fig. 11 Cutting force aviation versus hole number (cutting speed, 100 m/min; tangential feed, 0.04 mm/tooth; axial feed, 0.2 mm/rev)

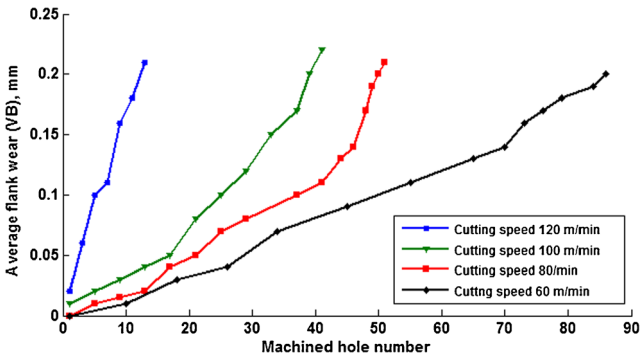

Fig. 12 Flank wear versus hole number at various cutting speeds (tangential feed, 0.04 mm/z; axial feed, 0.2 mm/rev)

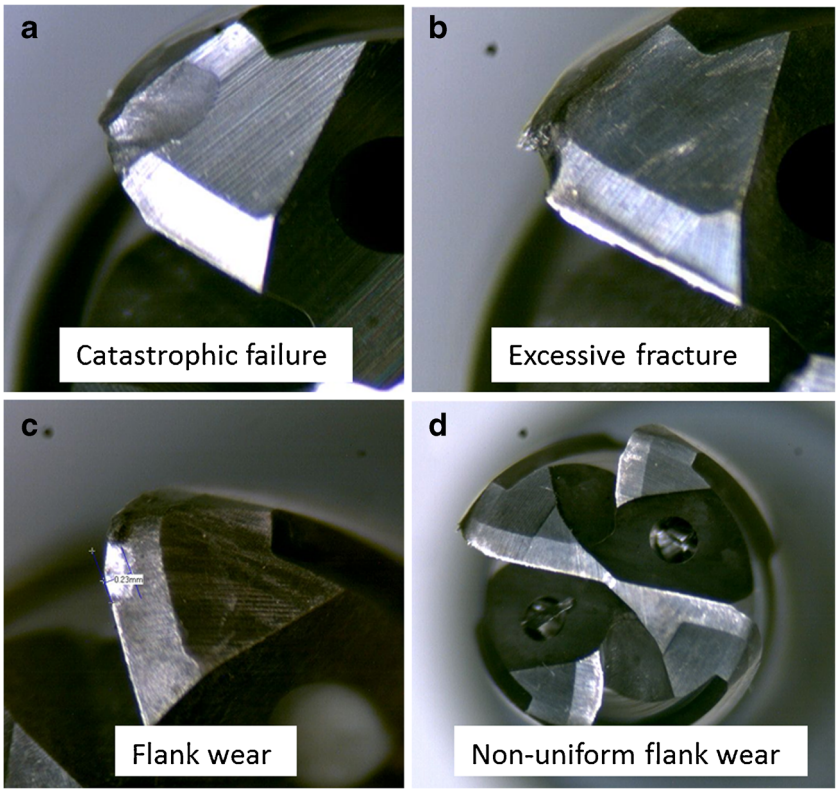

Fig. 13 Tool wear modes at the end of tool life under various cutting speeds (**a** 120 m/min, **b** 100 m/min, **c** 80 m/min, **d** 60 m/min)

mechanical damage, thermal damage, and adhesion [31]. As shown in the figure, thermal damage increases rapidly with increasing cutting speed. At higher cutting speed, chemical reaction and diffusion weaken the tool surface and make coating flaking and micro-chipping happened. These would increase the mechanical stresses and expose the tool substrate to the extremely worse cutting environment, and increase the catastrophic failure risk of the machining tool.

3.2 Quality of machined hole

Machining conditions which lead to poor quality of machined hole in the hole-making process are aggravated with increase of tool wear. The quality of machined holes presented in this paper includes geometrical accuracy, burr formation, and surface roughness.

3.2.1 Geometrical accuracy

Diameter accuracy and roundness tolerance are two important evaluation indicators for the quality of the machined hole. In this paper, hole diameter and roundness error have been measured using coordinate measuring machine (CMM), and each item was measured four times separately at different height and orientation. There is a concern that the heat generated in the hole-making process, particularly from the severe tool wear, will lead to thermal expansion of tool and workpiece that will affect the diameter size and quality of the machined holes [32]. However, as shown in Fig. 15, there is no significant changes in diameter and roundness error were observed. All diameter measurement mean values ranged from 9.962 to 9.991 mm, and average values of roundness error ranged from 0.011 to 0.025 mm. These values corresponding to dimensional and geometrical tolerance were reasonable in the whole helical milling operations even when the catastrophic failure of tool occurred. This would lead to the conclusion that the tool wear might not cause excessive deviation of diameter and roundness

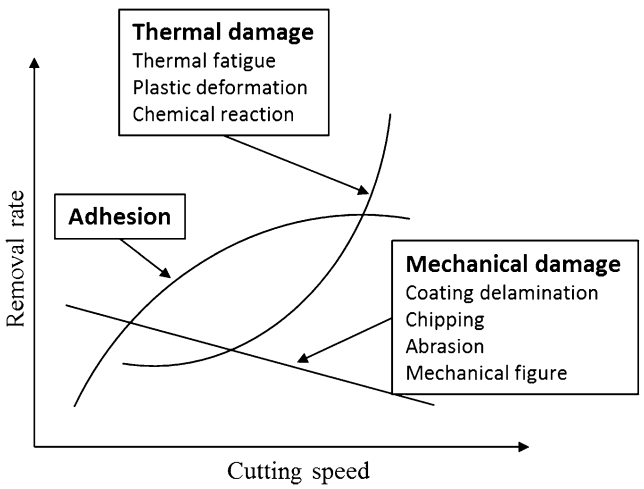

Fig. 14 Tool failure mechanisms versus cutting speed [31]

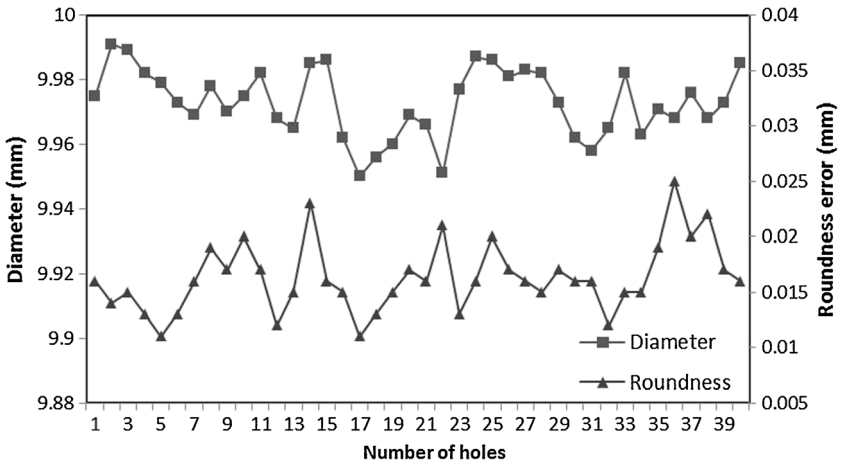

Fig. 15 Diameter and roundness error versus number of holes for dry helical milling

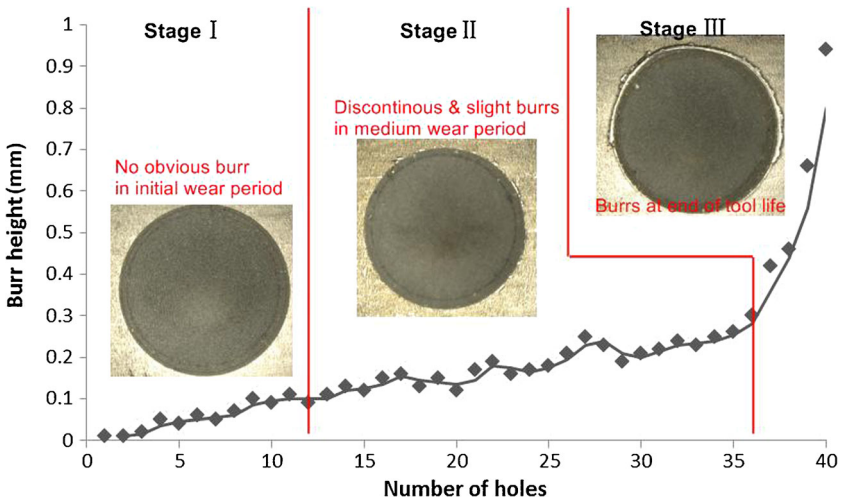

Fig. 16 Burr height at the exit of hole versus number of holes for dry helical milling

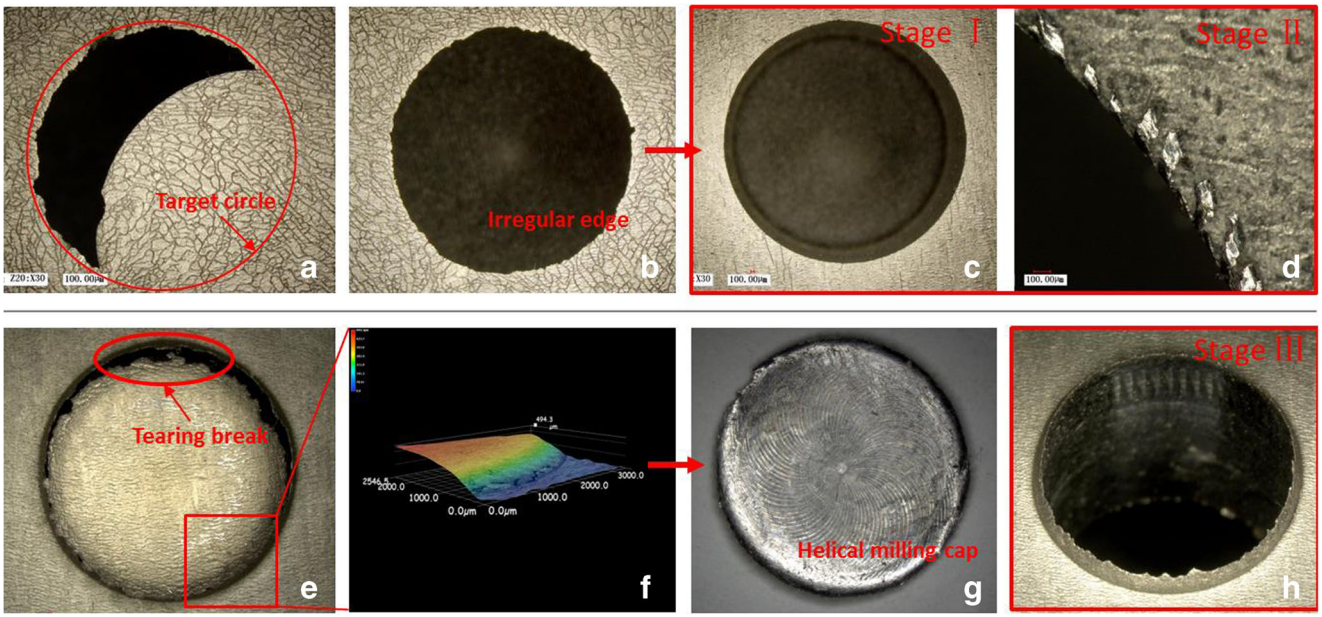

Fig. 17 Burr formation process at the exit of hole for three different stages: **a–c** initial wear of front cutting edge, corresponding to *stage I*; **a–e** burr formation process in medium wear of front cutting edge, corresponding to *stage II*; **e–h** burr formation at the end of tool life (*stage III*); **f** three-dimensional photo of helical milling cap

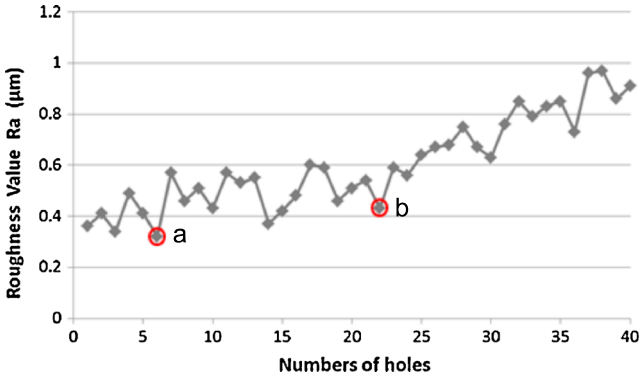

Fig. 18 Surface roughness measurements

error in the helical milling hole-making process. Owing to the feed, normal forces act on the tool center point and deflect it in the direction of the bore hole center point, and the actual diameter deviations are negative compared with the programmed target diameter [15].

3.2.2 Burr formation in dry helical milling of Ti-6Al-4V

Burrs in the machined holes cause fastener and material problems. Burrs would cause stress to be concentrated at the edges of holes, decreasing resistance to fracture and shortening fatigue life. Figure 16 shows the evolution of burr height at the exit of the hole versus the number of machined holes. According to the height and shape of the burr, the whole hole-making process can be divided into three stages, as shown in Fig. 16. In stage I, the value of burr height distributed in the range of 0∼0.1 mm, no obvious burr was observed in this stage. The burr height in stage II is in the range of 0.1∼0.3 mm, and the discontinuous and slight burrs can be observed at the edge of holes. The thickness of the burr in stage II is much smaller compared with that in stage III, and these burrs are easy to be removed. In stage III (as the number of machined hole passed the 36th hole), burr height increased rapidly and presented excessive values up to tool failure.

There are three types of burr that can be formed from machining operations: Poisson burr, rollover burr, and breakout burr [33]. Burrs may also be classified by the physical manner of formation. Plastic deformation of material includes lateral flow (Poisson burr), bending (rollover burr) and tearing of material from the workpiece (tear burr). As shown in Fig. 17a, the exit of the machined hole presented a crescent shape when the helical milling operation was almost getting to the end. The irregular edge can be observed when the front cutting edge (section B, shown in Fig. 3) was worn badly, but this irregular edge was not the final target circle; the final burr status of the hole exit depends on the wear condition of machining tools. In stage I, the residual workpiece of the irregular edge can be cut off by the corner of the cutting edge (section A, shown in Fig. 3) and the periphery cutting edge (section C, shown in Fig. 3) in the subsequent cutting process. As shown in Fig. 17c, no obvious burr can be observed in stage I because of the favorable cutting performance of the machining tool. However, the serious crater wear occurred at the tool nose (section A) with the increase of cutting times in stage II. This will cause lateral flow and bending when the irregular edge of the exit of the hole has been cut by worn front cutting edge and would lead to the rollover burr appearance at the exit of the hole, as shown in Fig. 17d. The helical milling cap appeared owing to the catastrophic failure at the front cutting edges with the increasing cutting time. As shown in Fig. 17e, f, the workpiece material was extruded out by the machining tool, instead of cutting them off, and then the large plastic deformation happened at the exit of the hole. When the thrust force reached the fracture limit of the workpiece material, the tearing break occurred at the boundary of the cap, and these led to the tear burr to happen in stage III, as shown in Fig. 17h.

3.2.3 Surface finish

Surface roughness was measured in three different generatrixs of each machined hole using Taylor roughness measuring instrument, a number of readings were taken, and the averages are detailed in Fig. 18. The average roughness (Ra) was approximately 0.4 μm in initial holes. Roughness increased at a cutting time corresponding to medium wear

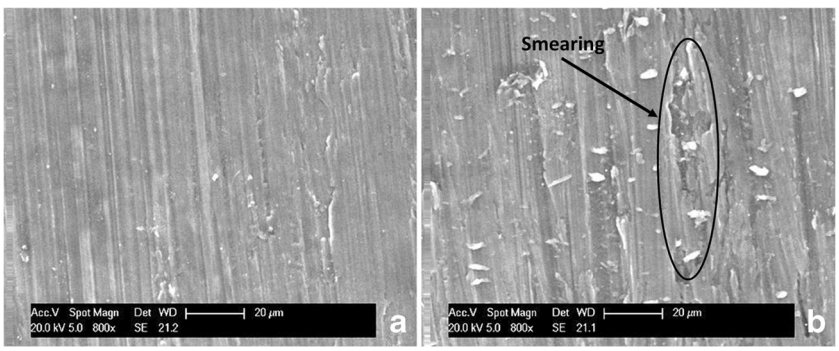

Fig. 19 Surface of the machined hole: **a** cutting time of 5 min, **b** cutting time of 18.3 min

of the tool, ranging from 0.4 to 0.8 μm. Finally, close to tool failure, roughness increased up to 1 μm. In the whole helical milling process, the evolution of surface roughness of holes was relatively smooth, and the reason for this was smooth wear that happened at the periphery cutting edge (section C) which mainly decides the hole surface finish in helical milling process. As shown in the figure, good surface roughness was obtained up to tool failure (the maximum mean value of surface roughness was 0.96 μm).

The surfaces of the machined holes were observed by SEM both in the cutting time of 5 and 18.3 min, in which chipping/fracture did not occur in the periphery cutting edge at the first time point (5 min, the sixth hole), but occurred at the second time point (18.3 min, the 22nd hole). A visual examination of all the holes showed clearly that micro-smearing can be observed in some locations of the machined hole surface when the chipping/fracture happened (even though surface roughness was not always significantly affected), compared with Fig. 19a, b. Smearing is unacceptable to the aerospace industry because it may cover cracks and other surface defects leading to premature in-service failure of the component. From Fig. 19, we can know that the surface quality with the cutting time of 5 min is better than that in the cutting time of 13.8 min, but their surface roughness values almost kept in the same level, as red-marked circle (a and b) shown in Fig. 18. Therefore, surface roughness could not fully characterize the quality of the machined surface in hole-making process. When chipping/fracture and flaking occurred, many small hard particles of tool substrate were generated. Smearing in the machined surface might occur owing to the existence of these hard particles of tool substrate, and the breakage of periphery cutting edge will lead to the irregular cutting marks at the same time.

4 Conclusions

This paper is focused on dry helical milling of Ti-6Al-4V, studying on tool wear evolution and its influence on the quality of machined holes (including geometrical accuracy, burr formation, and surface roughness). Based on the results of experimental investigation, the following conclusions can be drawn:

1. Due to the different machine environments, the wear mechanisms of front cutting edge zone and periphery cutting edge zone was not the same. The severe fracture and crater were observed at bottom cutting edge zone; however, smooth wear at flank face was a predominant wear mechanism at the periphery cutting edge zone. The different wear characteristics of the front and periphery cutting edges will also cause different cutting force variation trends in thrust and horizontal directions. The thrust force has a positive correlation with tool wear propagation, and it can be used to monitor the tool wear of front cutting edges.
2. Most serious wear occurred at the tool nose, which was originated by a combined action of diffusion and adhesion. Tool failure usually occurred at tool nose in helical milling hole-making process owing to the highest cutting temperature and then followed by front cutting edge. The high cutting speeds cause the more severe thermal damage in helical milling and thereby increase the catastrophic failure risk of machining tool.
3. SEM-EDS analysis showed progressive loss of TiAlN coating and adhesion of workpiece material in the rake face. Diffusion and oxidation wear were both observed in the periphery cutting edge and tool nose from SEM-EDS analysis results.
4. Machined hole quality, evaluated from the items of dimensions, roundness errors, and surface roughness, is elevated even at the end of tool life. However, tool wear of front cutting edge and tool nose has a tremendous impact on the height and shape of the exit burr in helical milling process. Moreover, there are two kinds of burr that can be observed in dry helical milling of Ti-6Al-4V, including rollover burr and tear burr.
5. Surface roughness could not fully characterize the quality of machined surface in hole-making process. The excellent surface roughness was maintained up to the end of tool life, but smearing can also be observed at the surface of the machined holes.

Acknowledgments The authors are grateful for funding supports by the National Natural Science Foundation of China (51275345), Natural Science Foundation of Tianjin (11JCZDJC22800), National High Technology Research and Development Program of China (2013AA040104), and Seed Foundation of Tianjin University.

References

1. Boyer RR (1996) An overview on the use of titanium in the aerospace industry. Mater Sci Eng A 213(1-2):103–114
2. Molinari A, Musquar C, Sutter G (2002) Adiabatic shear banding in high speed machining of Ti6Al4V: experiments and modeling. Int J Plast 18(4):443–459
3. López de Lacalle LN, Pérez J, Llorente JI, Sánchez JA (2000) Advanced cutting conditions for the milling of aeronautical alloys. J Mater Process Tech 100(1-3):1–11
4. Kramer BM (1986) A comprehensive tool wear model. CIRP Annals Manuf Technol 35(1):67–70
5. Venugopal KA, Paul S, Chattopadhyay AB (2007) Growth of tool wear in turning of Ti-6Al-4V alloy under cryogenic. Wear 262(9–10):1071–1078
6. Wanigarathne PC, Kardekar AD, Dillon OW, Poulachon G, Jawahir IS (2005) Progressive tool-wear in machining with coated grooved tools and its correlation with cutting temperature. Wear 259(7–12):1215–1224

7. Zhang S, Li JF, Sun J, Jiang F (2010) Tool wear and cutting forces variation in high-speed end-milling Ti-6Al-4V alloy. Int J Adv Manuf Technol 46(1-4):69–78
8. Mantle AL, Aspinwall DK, Wollenhofer O (1995) Twist drill of gamma titanium aluminade intermetallics. In: Proceedings of the 12th conference of the Irish manufacturing committee. University College Cork. September 6–8, pp 229–236
9. Li AH, Zhao J, Luo HB, Pei ZQ, Wang ZM (2012) Progressive tool failure in high-speed dry milling of Ti-6Al-4V alloy with coated carbide tools. Int J Adv Manuf Technol 58(5–8): 465–478
10. Sun J, Guo YB (2009) Material flow stress and failure in multiscale machining titanium alloy Ti-6Al-4V. Int J Adv Manuf Technol 41(7–8):651–659
11. Özel T, Sima M, Srivastava AK, Kaftanoglu B (2010) Investigations on the effects of multi-layered coated inserts in machining Ti-6Al-4V alloy with experiments and finite element simulations. CIRP Annals - Manuf Technol 59(1):77–82
12. Chen G, Ren CZ, Yang XY, Jin XM, Guo T (2011) Finite element simulation of high-speed machining of titanium alloy (Ti-6Al-4V) based on ductile failure model. Int J Adv Manuf Technol 56(9–12):1027–1038
13. Qin XD, Chen SM, Liu WC (2009) Development and application of helical milling technology in the aviation manufacturing and assembly industry. Aeronaut Manuf Technol 6:58–60. (in Chinese)
14. Iyer R, Koshy P, Ng E (2007) Helical milling: an enabling technology for hard machining precision holes in AISI D2 toolsteel. Int J Mach Tools Manuf 47(2):205–210
15. Denkena B, Boehnke D, Dege JH (2008) Helical milling of CFRP-titanium layer compounds. CIRP J Manuf Sci Technol 1(2):64–69
16. Brinksmeier E, Fangmann S, Meyer I (2008) Orbital drilling kinematics. Prod Eng Res Devel 2(3):277–283
17. Li Z, Liu Q (2013) Surface topography and roughness in hole-making by helical milling. Int J Adv Manuf Technol 66(9–12):1415–1425
18. Wang HY, Qin XD, Ren CZ, Wang Q (2012) Prediction of cutting forces in helical milling process. Int J Adv Manuf Technol 58(9–12):849–859
19. Canteroa JL, Tardío MM, Canteli JA, Marcos M, Miguéle MH (2005) Dry drilling of alloy Ti-6Al-4V. Int J Mach Tools Manuf 45(11):1246–1255
20. Harris SG, Vlasveld AC, Doyle ED, Dolder PJ (2000) Dry machining commercial viability through filtered arc vapour deposited coatings. Surf Coat Technol 133–134:383–388
21. Herbert CRJ, Kwong J, Kong MC, Axintea DA, Hardy MC, Withers PJ (2012) An evaluation of the evolution of workpiece surface integrity in hole making operations for a nickel-based superalloy. J Mater Process Technol 212(8):1723–1730
22. Sharman ARC, Amarasinghe A, Ridgway K (2008) Tool life and surface integrity aspects when drilling and hole making in Inconel 718. J Mater Process Technol 200:424–432
23. Biermann D, Heilmann M, Kirschner M (2011) Analysis of the influence of tool geometry on surface integrity in single-lip deep hole drilling with small diameters. Procedia Eng 19:16–21
24. Wang Z (1997) Machining of aerospace superalloys with coated (PVD and CVD) carbides and self-propelled rotary tools. PhD Thesis. South Bank University, UK
25. Lin TR (2002) Cutting behaviour of a TiN-coated carbide drill with curved cutting edges during the high-speed machining of stainless steel. J Mater Process Technol 127(1):8–16
26. Sharman ARC, Dewes RC, Aspinwall DK (2001) Tool life when high speed ball nose end milling of Inconel 718. J Mater Process Technol 118(1–3):29–35
27. Nabhani F (2001) Machining of aerospace titanium alloys. Robot Comput-Integr Manuf 17(1–2):99–106
28. Min W, Youzhen Z (1988) Diffusion wear in milling titanium alloys. Mater Sci Technol 4(6):548–553
29. Astakhov VP (2004) The assessment of cutting tool wear. Int J Mach Tools Manuf 44(6):637–647
30. Ezugwu EO, Wang ZM (1997) Titanium alloys and their machinability—a review. J Mater Process Technol 68(3):262–274
31. Childs T, Maekawa K, Obikawa T, Yamane Y (2000) Metal machining: theory and applications. Wiley, New York
32. Bono M, Hi J (2001) The effects of thermal distortions on the diameter and cylindricity of dry drilled holes. Int J Mach Tools Manuf 41(15):2261–2270
33. Stephenson DA, Agapiou JS (1997) Metal cutting theory and practice. Marcel Dekker, New York, p 435